HHS Public Access

Author manuscript

Int J Cancer. Author manuscript; available in PMC 2016 June 01.

Published in final edited form as:

Int J Cancer. 2016 June 1; 138(11): 2665–2677. doi:10.1002/ijc.29992.

Cathepsin L inactivation leads to multimodal inhibition of prostate cancer cell dissemination in a preclinical bone metastasis model

Dhivya R. Sudhan[1], **Christine Pampo**[1], **Lori Rice**[1], and **Dietmar W. Siemann**[1,2]

[1]Department of Radiation Oncology, University of Florida Health Cancer Center, Gainesville, FL

[2]Department of Pharmacology and Therapeutics, College of Medicine, University of Florida, Gainesville, FL

Abstract

It is estimated that approximately 90% of patients with advanced prostate cancer develop bone metastases; an occurrence that results in a substantial reduction in the quality of life and a drastic worsening of prognosis. The development of novel therapeutic strategies that impair the metastatic process and associated skeletal adversities is therefore critical to improving prostate cancer patient survival. Recognition of the importance of Cathepsin L (CTSL) to metastatic dissemination of cancer cells has led to the development of several CTSL inhibition strategies. The present investigation employed intra-cardiac injection of human PC-3ML prostate cancer cells into nude mice to examine tumor cell dissemination in a preclinical bone metastasis model. CTSL knockdown confirmed the validity of targeting this protease and subsequent intervention studies with the small molecule CTSL inhibitor KGP94 resulted in a significant reduction in metastatic tumor burden in the bone and an improvement in overall survival. CTSL inhibition by KGP94 also led to a significant impairment of tumor initiated angiogenesis. Furthermore, KGP94 treatment decreased osteoclast formation and bone resorptive function, thus, perturbing the reciprocal interactions between tumor cells and osteoclasts within the bone microenvironment which typically result in bone loss and aggressive growth of metastases. These functional effects were accompanied by a significant downregulation of NFκB signaling activity and expression of osteoclastogenesis related NFκB target genes. Collectively, these data indicate that the CTSL inhibitor KGP94 has the potential to alleviate metastatic disease progression and associated skeletal morbidities and hence may have utility in the treatment of advanced prostate cancer patients.

Keywords

cathepsin L; prostate cancer; metastasis; bone resorption; KGP94

Correspondence to: Dhivya R. Sudhan, Cancer and Genetics, Research Complex, Room 485E, University of Florida, Gainesville, FL 32610, USA, Tel.: +001-352-273-8251, Fax: +001-352-273-8252, dhivyasudhan@ufl.edu.

Additional Supporting Information may be found in the online version of this article.

The authors have no conflict of interest to disclose.

Prostate cancer is the most prevalent cancer and the second leading cause of cancer related death amongst men in the United States. It is estimated that in the year 2015 alone, about 220,800 new cases will be diagnosed and 27,540 men will die of prostate cancer with the bulk of tumor burden in the bone at the time of death.[1] While the prognosis for patients with localized disease is highly favorable, the 1 and 5 year survival rates of prostate cancer patients with metastatic bone disease drops to 47% and 3% respectively.[2] Indeed, the extent of metastatic disease in the bone serves as a strong predictor of disease outcome.[3] Once the primary tumor cells have disseminated to the bones, the patient is no longer considered for a curative therapy and receives only palliative treatment. In addition to their deleterious effects on survival, bone metastases severely impinge on the quality of life of these advanced prostate cancer patients. Skeletal metastases inflict debilitating complications including intractable bone pain, pathological fractures due to bone deformities, nerve compression syndromes including paralysis and paresis due to impingement of spinal nerves and anemia due to bone marrow ablation.[4] Thus, treatments aimed at inhibiting bone metastasis and delaying the onset of skeletal complications are critical to improving the survival and quality of life of prostate cancer patients.

Tumor secreted proteases play a significant role in many stages of tumor cell dissemination including detachment from the primary site, degradation of interstitial matrices and basal lamina, intravasation and extravasation across the capillary/lymphatic system and activation of latent growth factors to promote colonization at the secondary site.[5,6] One such protease, Cathepsin L (CTSL), a key member of the cathepsin family of cysteine proteases, has emerged as a promising metastasis promoting target in strategies seeking to impede the metastatic process.[6] CTSL upregulation has been reported in a wide range of human cancers including, ovarian, renal and breast carcinoma.[7] In most normal cells CTSL is primarily present within the lysosomes where it is committed to housekeeping functions such as terminal degradation of intracellular and endocytosed proteins.[8] However, cancer cells possess the ability to shunt this lysosomal enzyme into the secretory pathway *via* a variety of mechanisms.[9,10] Transformation dependent CTSL secretion has been shown to aid metastatic dissemination of cancer cells through dissolution of cell adhesion molecules and proteolytic degradation of basal lamina and extracellular matrix barriers.[9,11] This enzyme further fuels the proteolytic cascade by activating latent pro-forms of other key metastasis promoting proteases such as matrix metalloprotease, pro-heparanase, urokinase plasminogen activator and other members of the cathepsin family.[12–14] Studies including our own have also shown that tumor secreted CTSL plays a pivotal role in hypoxia and acidosis triggered metastatic aggressiveness of cancer cells.[15,16] The importance of CTSL upregulation in tumor progression is further supported by a number of clinical studies reporting a strong correlation between tumor CTSL levels and metastatic incidence, disease relapse and overall survival.[17,18]

In addition to promoting cancer cell dissemination, CTSL may also contribute to the expansion of metastatic cells within the bone matrix and subsequent development of metastasis associated skeletal morbidities. Although normal bone remodeling is typically driven by the osteoclast specific protease cathepsin K (CTSK), in the presence of tumor secreted cytokines, osteoclastic CTSL activity increases several fold and the enzyme begins

to play a significant, non-redundant role in the process of pathological bone resorption.[19,20] Bone resorption not only provides room for the expansion of the neoplastic cell mass but also leads to the release of active growth factors from the bone matrix that support aggressive growth of metastases.[21] Conceivably, inhibition of CTSL function will disengage this vicious cycle and cause not only alleviation of bone resorption, but also decrease in the tumor burden.

Recently, Kumar and colleague tested a library of small molecule inhibitors of CTSL enzymatic activity. The lead molecule, 3-bromophenyl-3-hydroxyphenyl-ketone thiosemicarbazone (KGP94) is a reversible, competitive inhibitor with high and comparable selectivity toward CTSL and CTSK (IC_{50} <135 nM)[22,23] compared with cathepsin B (IC_{50} > 10,000 nM). Our previous findings have shown that KGP94 significantly impedes metastasis associated cancer cell attributes such as migration and invasion.[15] The goal of present studies was to evaluate the anti-metastatic and anti-bone resorptive efficacy of KGP94 in a prostate cancer bone metastasis model.

Material and Methods

Cell culture

PC-3ML is a metastatic subline isolated from prostate cancer PC-3 cells through *in-vivo* selection of bone metastases[24] and thus exhibits a high propensity to metastasize to the bones. PC-3ML, DU145, LNCaP, LNCaP derived C4-2B, and mouse pre-osteoclastic RAW264.7 cells were cultured in HAM's F12 nutrient mixture, Eagle's MEM, RPMI, T-media and DMEM media, respectively, supplemented with 10% FBS. Human lung microvascular endothelial cells (HMVEC-L) were cultured in EGM2 MV media supplied by Lonza (CC-3202).Cells were maintained at 37°C in a humidified atmosphere of 5% CO_2 in air.

Prostate qPCR array

CTSL expression levels in prostate cancer patients were determined by performing semiquantitative RT-PCR analysis on a TissueScan Prostate cancer panel (Origene HPRT0824) as per manufacturer's instructions. CTSL mRNA levels were normalized to β-actin and are shown as relative levels normalized to normal tissue pools.

CTSL knockdown

1.25×10^5 PC-3ML cells were seeded in a six well dish. Forty-eight hr later, the cells were transfected with CTSL shRNA plasmids (OriGene TG305172) using Lipofectamine LTX plus reagent (Invitrogen) as per manufacturer's instructions. Transfected clones were isolated through puromycin selection and expanded. CTSL knockdown efficiency was tested by performing western blot on whole cell lysates and ELISA on cell culture supernatants. Clones exhibiting greater than 80% knockdown efficiency were used for *in-vivo* and *in-vitro* studies.

Reagent

KGP94 was kindly provided by Dr. Kevin Pinney of Baylor University. For *in-vitro* assays, KGP94 was dissolved in sterile DMSO to obtain a stock concentration of 25 mM and stored at −20°C. For treatment, the stock was further diluted in cell culture medium to achieve a working concentration of 25 μM. for *in-vivo* assays, KGP94 was sonicated in a 10% Tween 80 solution in 1 M HEPES buffer until completely dissolved. The drug was then filter sterilized and stored at 4°C.

Bone metastasis assay

All *in vivo* experiments were approved by the Institutional Animal Care and Use Committee (IACUC) of the University of Florida. 1×10^5 luciferase and GFP labeled PC-3ML cells were inoculated into the left ventricle of the heart of anesthetized athymic NCR nu/nu male mice. Mice received daily treatment of 20 mg/kg KGP94 (at 10 μL/g) *via* intraperitoneal (IP) injections. Bone metastasis was monitored on a weekly basis using the Xenogen IVIS imaging system by measuring photon flux 30 min after IP administration of D-Luciferin. For survival analysis, animals were euthanized when their meta-static burden reached an experimental endpoint of 1×10^9 photons/sec bioluminescence.

Histomorphometric analysis

Mice were arranged in the order of their bioluminescence intensity from highest to lowest signal intensity and those with the median bioluminescence intensity values from each group were selected for histological evaluation. Mice were euthanized and metastases bearing bones (determined based on bioluminescence signal) were harvested and fixed in 10% neutral buffered formalin solution for 24 hr. The bones were then washed with phosphate buffered saline (PBS) and decalcified in 10% EDTA solution for a week at 4°C. After complete decalcification, the bones were kept in a 30% sucrose solution overnight followed by OCT embedding. GFP positive areas were imaged using a Leica MZ 16 F camera.

Intradermal assay

1×10^5 PC-3ML cells were injected intradermally at four sites on the ventral surface of athymic NCR nu/nu male mice. One drop of trypan blue solution was added to impart a light blue color to the cell suspension and thus allow easy location of the site of cancer cell inoculation. A dose of 10 or 20 mg/kg KGP94 was administered IP on a daily basis. Three days later, the mice were euthanized and their skin flaps were removed and promptly analyzed. Tumor angiogenesis was evaluated by counting the number of blood vessels growing into the tumor nodule using a Zeiss Stemi SV 6 dissecting microscope.[25] Tumor nodule images were captured using a Leica MZ 16 F camera and Leica Application Suite software.

Invasion assay

PC-3ML (4×10^4), C42B (1×10^4), LNCaP (1.5×10^4), DU145 (1×10^4) or HMVEC-L (1×10^4) cells were suspended in serum free media and seeded into matrigel coated invasion inserts (BD Biosciences, 354480). For experiments testing the effect of pharmacological inhibition of CTSL, equal concentrations of KGP94 were added to the top and the bottom

chamber. Twenty-four hr later, non-invaded cells in the top chamber were scraped off using cotton tips. Invaded cells were fixed stained with crystal violet and enumerated under a microscope.

Tube formation assay

HMVEC-L cells (5×10^4) were seeded in a 24 well dish pre-coated with matrigel. The cells were incubated at 37°C in the presence of indicated concentrations of purified CTSL, KGP94 or tumor cell conditioned media. Ten hours later, tube structures were quantified and imaged using a Leica DMI 4000 B microscope.

Osteoclast formation and tartarate resistant acid phosphatase staining

For tartarate resistant acid phosphatase (TRAP) staining, 2.85×10^5 RAW 264.7 cells were seeded in a 24 well plate in the presence of indicated concentrations of RANKL (R&D systems) and KGP94 or purified CTSL (Calbiochem). Four days later, the cells were fixed and stained for TRAP using the acid phosphatase, leukocyte kit (Sigma Aldrich) as per manufacturer's instructions. TRAP positive multinucleate osteoclasts were quantified under a Zeiss Stemi SV 6 dissecting microscope and imaged using a Leica DMI 4000 B microscope.

For osteoclastogenesis gene expression analysis, 1.425×10^6 RAW 264.7 cells were seeded in a six well plate in the presence of indicated concentrations of RANKL, KGP94 or purified CTSL. Osteoclastogenesis marker expression was assessed every 24 hr for 4 days. For experiments assessing the effect of CTSL co-stimulation, gene expression analysis was performed 48 hr after RANKL and CTSL addition. For RNA extraction, cells were rinsed with PBS and lysed with TRIzol reagent (ThermoFisher Scientific). RNA was eluted using 100% isopropyl alcohol. Total RNA content was quantified using a ND-1000 spectrophotometer and reverse transcribed using Taqman reverse transcription reagents (ThermoFisher Scientific) as per manufacturer's instructions. The list of primers used to amplify cDNA of interest is shown in Supporting Information Table 1. Relative gene expression was determined by performing quantitative PCR using StepOne Real-Time PCR system (ThermoFisher Scientific).

Pit formation assay

Thick 100-μm slices of bovine cortical bone were sterilized with 70% ethanol, rinsed with sterile deionized water followed by overnight equilibration in DMEM media. Bone slices were then overlaid with 2.85×10^5 RAW 264.7 cells in the presence of 35 ng/mL RANKL and 25 μM KGP94. Four days later, the osteoclasts were scraped off the bone slices using a cotton swab. Bone slices were then rinsed in PBS and resorption pits were stained using 1% toluidine blue solution in 0.5% tetraborate. Resorption pits were imaged using a Zeiss Axioplane 2 imaging system and pit area was quantified using ImageJ software by calculating the area of toluidine positive region for each field of view at 10 × magnification. Four random fields were captured from each bone slice and four bone slices were tested under each experimental condition. Extent of bone resorption is expressed in terms of percent area of bone that was positively stained.

NFκB pathway analysis

RAW 264.7 cells were treated with or without 25 μM KGP94. One hr later, cells were stimulated with 35 ng/mL RANKL for indicated durations, lysed and processed for western blot analysis as previously described.[15] Densitometry analyses were carried out to determine band intensity using ImageJ software.

Cathepsin secretion analysis

To evaluate CTSL secretion during osteoclastogenesis, 3×10^6 RAW 264.7 cells were plated in 60 mm dishes in the presence or absence of 35 ng/mL RANKL. Cell culture supernatants were harvested at 24, 48 and 72 hr and centrifuged at 1,000 rpm for 10 min to remove any cell debris. Similarly, 24 hr conditioned media were harvested from PC-3ML, DU145, LNCaP and C42B prostate cancer cell lines. Secreted cathepsin levels in cell free supernatants were analyzed by performing enzyme linked immunosorbent assay using a Cathepsin L kit (human—R&D systems, DY952; mouse—My Biosource, MBS280424) and Cathepsin K kit (My Biosource MBS034890) as per manufacturers' instructions.

Viability assay

4.8×10^4 RAW 264.7 cells were seeded in a 96 well dish in the presence or absence of various concentrations of KGP94 or purified CTSL. Three days later, the cell culture medium was replaced with WST-1 [2-(4-Iodophenyl) −3-(4-nitrophenyl) −5-(2,4-disulfophenyl)−2H–tetrazolium, monosodium salt] reagent (Dojindo) in phenol red free medium. Four hr later viability was determined by measuring formazan dye formation at 450 nm using the Spectramax M5 (Molecular Devices) spectrophotometer.

Results

KGP94 treatment leads to a significant reduction in metastatic tumor burden and an overall improvement in survival

CTSL semi-quantitative RT-PCR using Tissuescan prostate tissue panels show an increase in CTSL transcript level in tumor samples from advanced stage patients (Fig. 1*a*). Similarly, elevated CTSL secreted levels were observed across prostate cancer cell lines derived from brain (DU145), lymph node (LNCaP) and bone (PC-3ML, C4-2B) metastases (Fig. 1*b*). To validate the importance of CTSL in tumor metastasis, CTSL knockdown PC-3ML cells were generated and clones exhibiting greater than 80% knockdown efficiency (Supporting Information Figs. 1*a* and 1*b*) were selected for testing the effect of CTSL deficiency on metastatic phenotype. While CTSL knockdown clones did not exhibit any change in proliferation (Supporting Information Fig. 1*c*), their invasive capacities were significantly impaired (Figs. 1*c* and 1*d*). CTSL deficient LNCaP cells showed a similar reduction in their invasive potential (Supporting Information Fig. 2). Since approximately 90% of advanced prostate cancer patients suffer from bone metastases and associated skeletal morbidities,[26] the focus of this investigation was to determine the anti-metastatic efficacy of CTSL targeting in a bone metastasis model. To validate the importance of CTSL in the PC-3ML bone metastasis model, empty vector or CTSL shRNA transfected PC-3ML cells were injected *via* the intracardiac (IC) route and metastatic progression was monitored by weekly

bioluminescence imaging using the firefly luciferase reporter system. Compared with empty vector controls, CTSL knockdown led to a significant reduction in metastatic burden (~98% reduction) (Figs. 1*e* and 1*f*) and improvement in overall survival (Fig. 1*g*).

Prostate cancer models PC-3ML, DU145, LNCaP and C4-2B secrete CTSL (Fig. 1*b*) but little or no CTSK (Supporting Information Fig. 3) (1387 *vs*. 24 pg/mL; 1232 *vs*. 1.8 pg/mL; 360 *vs*. 3.2 pg/mL and 638 *vs*. 3.3 pg/mL, respectively). Treatment with the small molecule inhibitor KGP94 suppressed the activity of secreted CTSL[15] and significantly impaired the invasive capacities of various metastatic prostate cancer cell lines (Supporting Information Fig. 4) without exerting any cytotoxic effects.[15] To assess the anti-metastatic efficacy of this agent *in vivo*, mice were injected (IC) with PC-3ML cells and then treated daily with 20 mg/kg doses of KGP94. Metastatic progression in control and treated mice was monitored by weekly bioluminescence imaging. The results showed that KGP94 treatment led to a significant reduction (65%) in metastatic tumor burden and an improvement in the overall survival of metastases bearing mice (Figs. 2*a*–2*c*). Histological assessments based on GFP imaging and hematoxylin and eosin staining confirmed that the reduction in bioluminescence signal in KGP94 treated mice was attributable to a decrease in tumor burden (Fig. 2*d*). Quantification of bone lesions revealed that KGP94 mediated reduction in metastatic burden was at least in part due to a significant decrease in the number of metastatic foci (Fig. 2*e*). Although PC-3ML cells predominantly form skeletal metastases, occasional soft tissue metastases also were observed (Fig. 2*f*). A reduction in soft tissue metastases in KGP94 treated mice was noted but the difference was not statistically significant.

CTSL inhibition impairs the angiogenic capacity of prostate cancer cells

To test whether suppression of angiogenesis could have contributed to the reduction in tumor burden resulting from KGP94 treatment, PC-3ML cells were inoculated intradermally, and the effect of KGP94 exposure on tumor induced blood vessel formation was determined (Figs. 3*a* and 3*b*). The results showed that compared with untreated controls, mice that were treated with either 10 or 20 mg/kg KGP94 showed a significant reduction in tumor angiogenesis as demonstrated by a dose dependent decrease in the number of tumor induced blood vessels (31% and 58% decrease, respectively). Similarly, CTSL knockdown PC-3ML cells induced 72% fewer blood vessels compared with PC-3ML cells transfected with an empty vector. However, KGP94 treatment of mice inoculated with CTSL knockdown PC-3ML cells did not exert any effect on tumor vessel count (Supporting Information Fig. 4). *In vitro* assessment of the effect of KGP94 on various pro-angiogenic functions such as invasiveness and tube forming capacity of endothelial cells showed that while KGP94 had no apparent effect on naïve endothelial cells, it led to a significant reduction in purified CTSL stimulated endothelial cell invasion and tube formation (Figs. 3*c*–3*e*). Similarly, endothelial cells that were incubated with conditioned media derived from CTSL knockdown PC-3ML or LNCaP (Supporting Information Fig. 5) cells showed a striking decrease in their angiogenic properties compared with those stimulated with conditioned media harvested from empty vector transfected cells.

KGP94 suppresses the bone resorptive capacity of osteoclasts

Progressive growth of bone metastases is strongly dependent on reciprocal interactions between cancer cells and bone resorbing osteoclasts and bone forming osteoblasts.[27] Both osteolytic and osteoblastic metastases secrete osteoclast activating cytokines leading to bone resorption and release of growth factors from the bone matrix. These growth factors in turn stimulate tumor cell proliferation and further cytokine release. Thus disengagement of osteoclastic function would not only alleviate skeletal complications but would make bone a less favorable niche for metastatic expansion. Moreover, CTSL has been widely implicated to participate in pathological bone resorption.[28] To test whether KGP94 treatment could disrupt osteoclast mediated bone resorption by interfering with osteoclast formation or the osteolytic function of mature osteoclasts, the impact of KGP94 was evaluated in murine pre-osteoclastic RAW 264.7 cells. Tumor secreted cytokines promote osteoblastic secretion of Receptor activator of nuclear kappa-B ligand (RANKL); an essential mediator of osteoclast formation and activity. Upon exposure to RANKL, RAW 264.7 cells underwent fusion and differentiation to form multinucleate, TRAP positive osteoclasts (Figs. 4*a* and 4*b*). However, in the presence of KGP94, a significant decrease in the number of mature osteoclasts was observed. These results were further substantiated by a significant reduction in the phosphorylation levels of IKK and IκB, which are key mediators of RANKL stimulated NFκB signaling cascade (Fig. 4c). Moreover, KGP94 treatment also led to a significant reduction in the expression of osteoclastogenesis related NFκB target genes such as calcitonin receptor and RANK (Figs. 4*d* and 4*e*). This reduction in osteoclast formation was not due to a cytotoxic effect of KGP94 (Fig. 1*f*). In mature osteoclasts, compared with the RANKL alone controls, RAW264.7 cells stimulated with RANKL in the presence of KGP94 showed a significantly reduced bone pit forming capacity as demonstrated by a decrease in O-toluidine staining intensity (Figs. 4*g* and 4*h*). These data collectively suggest that KGP94 affects bone resorption by inhibiting both osteoclast formation and the osteolytic activity of mature osteoclasts.

CTSL promotes osteoclast formation

While the role of CTSL in pathological osteoclastic function is well recognized, its involvement in the osteoclast formation process remains less explored. Conditioned media analysis revealed that RANKL stimulated osteoclast formation was accompanied by a significant increase in CTSL secretion (Fig. 5*a*). To test whether CTSL can promote osteoclastogenesis a dose response analysis with various concentrations of RANKL was performed and sub-optimal RANKL doses were identified (Fig. 5*b*). The results showed that co-stimulation of RAW264.7 cells with CTSL and sub-optimal concentrations of 1 or 5 ng/mL of RANKL led to a significant increase in the expression of osteoclastogenesis marker genes (Figs. 5*c* and 5*d*) and the number of mature TRAP+ multinucleate osteoclasts formed (Figs. 5*f* and 5*g*). Interestingly, the extent of osteoclast formation in the combination group was greater than that observed for saturating concentration of 35 ng/mL of RANKL alone. Viability assays revealed that the increase in osteoclast formation was not due to an effect on cell proliferation (Fig. 5*e*).

Discussion

First line treatment for prostate cancer consists of radical prostatectomy or radiation coupled with androgen deprivation therapy. Although these treatments are highly effective initially, nearly one-third patients eventually suffer from local or metastatic recurrence.[29] Approximately 90% of these advanced prostate cancer patients develop bone metastases at which point the disease is considered highly incurable.[26] While the new generation anti-resorptive agents such as bisphosphonates, RANKL quenchers, and cathepsin K inhibitors provide effective palliative care and reduce morbidity, they exhibit little if any anti-metastatic efficacy.[30,31] Thus novel therapeutic agents that can serve both as effective anti-metastatic agent and active anti-resorptive therapy are highly desired. The ability of CTSL to influence several critical aspects of malignant tumor progression such as metastatic aggressiveness, drug resistance, disease relapse and skeletal morbidities makes it an ideal candidate for therapeutic intervention.[11,17,32,33] Promising outcomes of various CTSL targeting approaches ranging from gene knockout to ectopic expression of endogenous inhibitors or antisense, at curbing tumor progression and metastatic disease, place further emphasis on the importance of development and pre-clinical evaluation of effective CTSL targeting agents.[11,34,35] To date, the development of CTSL specific inhibitors has been hampered by the high degree of structural homology between different members of the cathepsin family.[36] The present study investigates the anti-metastatic efficacy of a thiosemicarbazone based CTSL inhibitor KGP94, which impairs CTSL proteolytic function by targeting its active site.[37]

Elevated CTSL secreted levels were observed across prostate cancer cell lines derived from brain (DU145), lymph node (LNCaP) and bone (PC-3ML, C4-2B) metastases (Fig. 1*b*). Even though the bone metastatic capacity of DU 145 cells is significantly lower compared with PC-3ML cells, they secreted relatively same amounts of CTSL. Since tropism to different metastatic sites is influenced by a repertoire of several different oncogenes, despite the similarity in CTSL secretion, their tropism varies due to their vastly different gene expression profiles.

CTSL knockout studies in a spontaneous pancreatic carcinogenesis model reported that CTSL deficiency retards tumor growth and significantly hampers the progression of benign encapsulated tumors into invasive carcinomas thus indicating that CTSL plays a key role in the process of tumor invasion and metastasis.[11] Further, KGP94 mediated CTSL inhibition has been shown to result in a substantial inhibition of tumor microenvironment potentiated metastatic capacity of cancer cells.[15] In agreement with these findings, our present study shows that CTSL inactivation by shRNA knockdown resulted in a significant suppression of prostate cancer cell dissemination to bone (Figs. 1*e* and 1*f*). Importantly, CTSL targeting with the small molecule CTSL inhibitor KGP94 resulted in a significant reduction in metastatic incidence, tumor burden and a resultant improvement in the overall survival of KGP94 treated mice.

Since successful establishment of metastases is contingent on effective execution of several different processes such as invasion through the interstitium to arrive at the secondary site, initiation of angiogenesis to support the growth of the newly formed metastatic lesion and

establishment of a constructive interaction with the new microenvironment; disruption of any of these processes could result in a similar decline in metastatic burden. Our prior studies established that KGP94 treatment could effectively impair PC-3ML migration and invasion[27] and the present investigation confirms the inhibitory effects on metastatic cell phenotype in three other prostate cancer cell models (Supporting Information Fig. 4). In addition, both pharmacological and genetic ablation of CTSL leads to a significant reduction in the ability of PC-3ML tumor cells to induce blood vessels (Fig. 3). Importantly, KGP94 treatment of CTSL knockdown PC-3ML cancer cells did not result in additional reduction in the angiogenic capacity of these cancer cells (Supporting Information Fig. 6) further supporting the notion that CTSK does not participate in tumor angiogenesis.

Although the role of CTSL in tumor angiogenesis remains poorly understood, observations made in other pathological disorders are strongly suggestive of its proangiogenic function.[38,39] Rebbaa *et al*. have demonstrated that CTSL inhibition significantly suppressed angiogenesis by repressing endothelial cell extracellular matrix digestive capacity.[39] Furthermore, highly potent pro-angiogenic factors such as VEGF and bFGF have been shown to induce CTSL expression and secretion to stimulate mitogen activated protein kinase pathways in endothelial cells in a paracrine fashion.[38] Importantly, the contribution of CTSL to bFGF stimulated angiogenesis in ischemic disease models was far greater than that noted for other well recognized proteases such as matrix metallo-protease 1 and plasminogen activator inhibitor-1. Thus, CTSL could contribute to the process of tumor angiogenesis by extracellular matrix digestion to assist endothelial cell invasion through the interstitium, or, through more complex mechanisms involving activation of pro-angiogenic signaling pathways.

It has been observed that in prostate cancer patients with skeletal metastases, tumor cells alter the local cytokine milieu leading to unrestrained activation of osteoclasts as demonstrated by a significant elevation in biomarkers of bone resorption.[40] These cytokines have been shown to selectively upregulate osteoclastic CTSL synthesis in order to promote active resorption of bone matrix components including type I collagen.[33,41] Such osteolytic events in turn release several active growth factors stored within the bone matrix to support aggressive growth of metastases.[42] In the present investigation we demonstrated that KGP94 treatment actively interferes with osteoclastic bone resorption (Fig. 4), thereby suggesting that KGP94 could have manifested its anti-metastatic activity, at-least in part, by interfering with the tumor-bone microenvironment interplay. These findings are in agreement with observations made in other pathological conditions involving CTSL. For example, steroidal hormones such as estrogens protect bone health by negatively regulating osteoclastic synthesis of CTSL.[43] Thus, CTSL knockout mice displayed a marked resistance to osteoporosis upon ovariectomy.[44] Pharmacological intervention of CTSL also yielded similar suppression of bone resorption in osteoporotic mice.[45] In addition to the anticipated decline in bone resorption, KGP94 also led to a drastic impairment of the osteoclast formation process (Fig. 4). While of role of CTSL in osteoclastic function is well documented, the mechanism through which CTSL inhibition affects osteoclast formation is not nearly as clear. In addition to their anti-collagenolytic function, administration of CTSL specific inhibitor to ovariectomized mice also inhibited calcium release from the bone.[46]

During osteoclastic bone resorption, acidification of the resorption lacuna dissolves the mineral component of the bone which exposes the collagen rich organic matrix for digestion by cathepsins and other proteases. Since dissolution of the mineral component of the bone is independent of the proteolytic function of osteoclasts, this decline in calcium level implicates of a decrease in osteoclast formation. In order to validate the observations on osteoclast formation in the presence of KGP94, CTSL secretion and its effect on osteoclastogenesis were tested. RANKL stimulated differentiation of pre-osteoclastic RAW 264.7 cells was accompanied by a striking increase in secreted CTSL levels. While purified CTSL alone had no impact on RAW 264.7 cell proliferation or differentiation, combined exposure of CTSL with sub-optimal concentrations of RANKL led to a striking increase in osteoclastogenesis approaching that seen by treatment with 35 ng/mL of RANKL (Fig. 5). The ability of purified CTSL to augment RANKL stimulated osteoclastogenesis thus further underscores the involvement of CTSL in the differentiation process perhaps in a catalytic capacity.

Since KGP94 exhibits similar selectivity against CTSL and CTSK, some of its anti-metastatic effect could, at least in part, be attributed to its anti-CTSK activity. CTSK is an osteoclast specific protease and is predominantly involved in normal and pathological bone remodeling.[47] While its inhibition would not affect neoplastic cell or angiogenic function of endothelial cells, it could result in a reduction in bone tumor burden due to disruption of the "vicious cycle" between tumor cells and osteoclasts. Studies in $CTSK^{-/-}$ mice have clearly demonstrated that CTSK does not participate in the osteoclast formation process and thus the reduction in bone tumor burden is purely mediated through inhibition of resorptive function of mature osteoclasts.[48] Our studies, on the other hand show that CTSL promotes osteoclast formation process (Fig. 5) which is effectively inhibited in the presence of KGP94 (Fig. 4). Moreover, bone metastasis study using CTSL knockdown PC-3ML cells further validates the efficacy of CTSL inhibition strategies at decreasing metastatic burden in the bone (Fig. 1). Taken together our studies suggest that while the inhibitory effects of KGP94 on the neoplastic cell metastatic phenotype and ability to induce angiogenesis are the consequence of suppression of secreted CTSL activity, its suppression of bone remodeling could be a consequence of both CTSL and CTSK activity inhibition, Thus CTSL inhibitors with anti-CTSK activity could potentially yield better clinical outcomes impacting both neoplastic cell progression and alleviating bone morbidities by inhibiting both osteoclast formation and activity.

Even though skeletal metastases in prostate cancer patients are predominantly osteoblastic, this abnormal bone formation is mostly preceded by osteolytic events thus indicating that bone resorption might be a prerequisite for abnormal osteoblastic activity.[49] In addition to cancer induced osteolysis, standard of care cytotoxic, glucocorticoid and androgen deprivation therapies have been proven to accelerate bone loss.[50] Hence, numerous anti-resorptive agents are actively being used in the clinic as palliative treatment for prostate cancer patients with bone metastases. Thus the anti-resorptive function of KGP94 coupled with its anti-metastatic activity would not only decrease metastatic incidence and patient mortality but could also improve the quality of life of these patients by averting skeletal morbidities.

In summary, KGP94 mediated CTSL inactivation resulted in a significant reduction in metastatic incidence, tumor burden and an improvement in overall survival. Mechanistically, this could be the consequence of anti-invasive, anti-angiogenic and anti-resorptive effects of KGP94 (Fig. 6). These findings suggest that selective cathepsin inhibition by the small molecule targeting agents such as KGP94 may have the potential to significantly alleviate metastatic disease progression and associated skeletal morbidities in prostate cancer patients.

Supplementary Material

Refer to Web version on PubMed Central for supplementary material.

Acknowledgments

The authors thank Dr. Kevin Pinney of Baylor University and OXiGENE Inc. for providing KGP94.

Grant sponsor: National Cancer Institute; **Grant number:** US Public Health Service Grant R01 CA169300

References

1. Siegel RL, Miller KD, Jemal A. Cancer statistics, 2015. CA: Cancer J Clin. 2015; 65:5–29. [PubMed: 25559415]
2. Norgaard M, Jensen AO, Jacobsen JB, et al. Skeletal related events, bone metastasis and survival of prostate cancer: a population based cohort study in Denmark (1999 to 2007). J Urol. 2010; 184:162–7. [PubMed: 20483155]
3. Soloway MS, Hardeman SW, Hickey D, et al. Stratification of patients with metastatic prostate cancer based on extent of disease on initial bone scan. Cancer. 1988; 61:195–202. [PubMed: 3334948]
4. Carlin BI, Andriole GL. The natural history, skeletal complications, and management of bone metastases in patients with prostate carcinoma. Cancer. 2000; 88:2989–94. [PubMed: 10898342]
5. Palermo C, Joyce JA. Cysteine cathepsin proteases as pharmacological targets in cancer. Trends Pharmacol Sci. 2008; 29:22–8. [PubMed: 18037508]
6. Lankelma JM, Voorend DM, Barwari T, et al. Cathepsin L, target in cancer treatment? Life Sci. 2010; 86:225–33. [PubMed: 19958782]
7. Chauhan SS, Goldstein LJ, Gottesman MM. Expression of cathepsin L in human tumors. Cancer Res. 1991; 51:1478–81. [PubMed: 1997186]
8. Barrett AJ, Kirschke H, Cathepsin B, Cathepsin H, cathepsin L. Methods Enzymol. 1981; 80(Pt C): 535–61. [PubMed: 7043200]
9. Gal S, Willingham MC, Gottesman MM. Processing and lysosomal localization of a glycoprotein whose secretion is transformation stimulated. J Cell Biol. 1985; 100:535–44. [PubMed: 3968177]
10. Stearns NA, Dong JM, Pan JX, et al. Comparison of cathepsin L synthesized by normal and transformed cells at the gene, message, protein, and oligosaccharide levels. Arch Biochem Biophys. 1990; 283:447–57. [PubMed: 2275556]
11. Gocheva V, Zeng W, Ke D, et al. Distinct roles for cysteine cathepsin genes in multistage tumorigenesis. Genes Dev. 2006; 20:543–56. [PubMed: 16481467]
12. Goretzki L, Schmitt M, Mann K, et al. Effective activation of the proenzyme form of the urokinase-type plasminogen activator (pro-uPA) by the cysteine protease cathepsin L. FEBS Lett. 1992; 297:112–8. [PubMed: 1551416]
13. Everts V, Korper W, Hoeben KA, et al. Osteoclastic bone degradation and the role of different cysteine proteinases and matrix metalloproteinases: differences between calvaria and long bone. J Bone Miner Res. 2006; 21:1399–408. [PubMed: 16939398]

14. Laurent-Matha V, Derocq D, Prebois C, et al. Processing of human cathepsin D is independent of its catalytic function and auto-activation: involvement of cathepsins L and B. J Biochem. 2006; 139:363–71. [PubMed: 16567401]
15. Sudhan DR, Siemann DW. Cathepsin L inhibition by the small molecule KGP94 suppresses tumor microenvironment enhanced metastasis associated cell functions of prostate and breast cancer cells. Clin Exp Metastasis. 2013; 30:891–902. [PubMed: 23748470]
16. Cuvier C, Jang A, Hill RP. Exposure to hypoxia, glucose starvation and acidosis: effect on invasive capacity of murine tumor cells and correlation with cathepsin (L + B) secretion. Clin Exp Metastasis. 1997; 15:19–25. [PubMed: 9009102]
17. Thomssen C, Schmitt M, Goretzki L, et al. Prognostic value of the cysteine proteases cathepsins B and cathepsin L in human breast cancer. Clin Cancer Res. 1995; 1:741–6. [PubMed: 9816040]
18. Xu X, Yuan G, Liu W, et al. Expression of cathepsin L in nasopharyngeal carcinoma and its clinical significance. Exp Oncol. 2009; 31:102–5. [PubMed: 19550400]
19. Kakegawa H, Tagami K, Ohba Y, et al. Secretion and processing mechanisms of procathepsin L in bone resorption. FEBS Lett. 1995; 370:78–82. [PubMed: 7649308]
20. Tagami K, Kakegawa H, Kamioka H, et al. The mechanisms and regulation of procathepsin L secretion from osteoclasts in bone resorption. FEBS Lett. 1994; 342:308–12. [PubMed: 8150090]
21. Roodman GD. Mechanisms of bone metastasis. N Engl J Med. 2004; 350:1655–64. [PubMed: 15084698]
22. Kumar GD, Chavarria GE, Charlton-Sevcik AK, et al. Functionalized benzophenone, thiophene, pyridine, and fluorene thiosemicarbazone derivatives as inhibitors of cathepsin L. Bioorg Med Chem Lett. 2010; 20:6610–5. [PubMed: 20933415]
23. Chavarria, GE. Kinetic characterization of Thiosemicarbazone as cysteine protease inhibitors and their potential use as therapeutic agents against metastatic cancer and Chagas disease. Waco, Texas: Baylor University; 2012.
24. Wang M, Stearns ME. Isolation and characterization of PC-3 human prostatic tumor sublines which preferentially metastasize to select organs in S.C.I.D. mice. Differentiation. 1991; 48:115–25. [PubMed: 1773917]
25. Siemann DW, Norris CM, Ryan A, Shi W. Impact of tumor cell VEGF expression on the in vivo efficacy of vandetanib (ZACTIMA;ZD6474). Anticancer Res. 2009; 29:1987–92. [PubMed: 19528456]
26. Bubendorf L, Schopfer A, Wagner U, et al. Metastatic patterns of prostate cancer: an autopsy study of 1,589 patients. Hum Pathol. 2000; 31:578–83. [PubMed: 10836297]
27. Raggatt LJ, Partridge NC. Cellular and molecular mechanisms of bone remodeling. J Biol Chem. 2010; 285:25103–8. [PubMed: 20501658]
28. Sudhan DR, Siemann DW. Cathepsin L targeting in cancer treatment. Pharmacol Ther. 2015; 155:105–16. [PubMed: 26299995]
29. Leventis AK, Shariat SF, Kattan MW, et al. Prediction of response to salvage radiation therapy in patients with prostate cancer recurrence after radical prostatectomy. J Clin Oncol. 2001; 19:1030–9. [PubMed: 11181666]
30. Fizazi K, Carducci M, Smith M, et al. Denosumab versus zoledronic acid for treatment of bone metastases in men with castration-resistant prostate cancer: a randomised, double-blind study. Lancet. 2011; 377:813–22. [PubMed: 21353695]
31. Fournier PG, Stresing V, Ebetino FH, et al. How do bisphosphonates inhibit bone metastasis in vivo? Neoplasia. 2010; 12:571–8. [PubMed: 20651986]
32. Zheng X, Chu F, Chou PM, et al. Cathepsin L inhibition suppresses drug resistance in vitro and in vivo: a putative mechanism. Am J Physiol Cell Physiol. 2009; 296:C65–C74. [PubMed: 18971393]
33. Leto G, Sepporta MV, Crescimanno M, et al. Cathepsin L in metastatic bone disease: therapeutic implications. Biol Chem. 2010; 391:655–64. [PubMed: 20370324]
34. Gianotti A, Sommer CA, Carmona AK, et al. Inhibitory effect of the sugarcane cystatin CaneCPI-4 on cathepsins B and L and human breast cancer cell invasion. Biol Chem. 2008; 389:447–53. [PubMed: 18208350]

35. Kirschke H, Eerola R, Hopsu-Havu VK, et al. Antisense RNA inhibition of cathepsin L expression reduces tumorigenicity of malignant cells. Eur J Cancer. 2000; 36:787–95. [PubMed: 10762753]
36. Turk V, Turk B, Turk D. Lysosomal cysteine proteases: facts and opportunities. Embo J. 2001; 20:4629–33. [PubMed: 11532926]
37. Kishore Kumar GD, Chavarria GE, Charlton-Sevcik AK, et al. Design, synthesis, and biological evaluation of potent thiosemicarbazone based cathepsin L inhibitors. Bioorg Med Chem Lett. 2010; 20:1415–9. [PubMed: 20089402]
38. Chung JH, Im EK, Jin TW, et al. Cathepsin L derived from skeletal muscle cells transfected with bFGF promotes endothelial cell migration. Exp Mol Med. 2011; 43:179–88. [PubMed: 21350328]
39. Rebbaa A, Chu F, Sudha T, et al. The anti-angiogenic activity of NSITC, a specific cathepsin L inhibitor. Anticancer Res. 2009; 29:4473–81. [PubMed: 20032394]
40. Coleman RE, Major P, Lipton A, et al. Predictive value of bone resorption and formation markers in cancer patients with bone metastases receiving the bisphosphonate zoledronic acid. J Clin Oncol. 2005; 23:4925–35. [PubMed: 15983391]
41. Leto MC, Flandina C, Sepporta MV, et al. Cathepsin L in Normal and Pathological Bone Remodeling. Clin Rev Bone Miner Metab. 2011; 9:109–21.
42. Yoneda T, Hiraga T. Crosstalk between cancer cells and bone microenvironment in bone metastasis. Biochem Biophys Res Commun. 2005; 328:679–87. [PubMed: 15694401]
43. Furuyama N, Fujisawa Y. Regulation of collagenolytic cysteine protease synthesis by estrogen in osteoclasts. Steroids. 2000; 65:371–8. [PubMed: 10899536]
44. Potts W, Bowyer J, Jones H, et al. Cathepsin L-deficient mice exhibit abnormal skin and bone development and show increased resistance to osteoporosis following ovariectomy. Int J Exp Pathol. 2004; 85:85–96. [PubMed: 15154914]
45. Woo JT, Yamaguchi K, Hayama T, et al. Suppressive effect of N-(benzyloxycarbonyl)-L-phenylalanyl-L-tyros in al on bone resorption in vitro and in vivo. Eur J Pharmacol. 1996; 300:131–5. [PubMed: 8741178]
46. Yasuma T, Oi S, Choh N, et al. Synthesis of peptide aldehyde derivatives as selective inhibitors of human cathepsin L and their inhibitory effect on bone resorption. J Med Chem. 1998; 41:4301–8. [PubMed: 9784105]
47. Le Gall C, Bonnelye E, Clezardin P. Cathepsin K inhibitors as treatment of bone metastasis. Curr Opin Support Palliat Care. 2008; 2:218–22. [PubMed: 18685424]
48. Leung P, Pickarski M, Zhuo Y, et al. The effects of the cathepsin K inhibitor odanacatib on osteoclastic bone resorption and vesicular trafficking. Bone. 2011; 49:623–35. [PubMed: 21718816]
49. Zhang J, Dai J, Qi Y, et al. Osteoprotegerin inhibits prostate cancer-induced osteoclastogenesis and prevents prostate tumor growth in the bone. J Clin Invest. 2001; 107:1235–44. [PubMed: 11375413]
50. Pfeilschifter J, Diel IJ. Osteoporosis due to cancer treatment: pathogenesis and management. J Clin Oncol. 2000; 18:1570–93. [PubMed: 10735906]

What's new?

A majority of advanced prostate cancer patients suffer from bone metastases and related skeletal morbidities, with no known cure. Cathepsin L (CTSL), a tumor secreted protease, has been clinically associated with metastatic disease incidence and progression in prostate cancer. The present study demonstrates that treatment with KGP94, a small-molecule inhibitor of CTSL, impairs various aspects of metastatic progression including incidence, disease burden, tumor-induced angiogenesis, and osteolysis in a pre-clinical prostate cancer model. The CTSL inhibitor KGP94, thus, has the potential to alleviate metastatic disease progression and associated skeletal morbidities and have utility in the treatment of advanced prostate cancer patients.

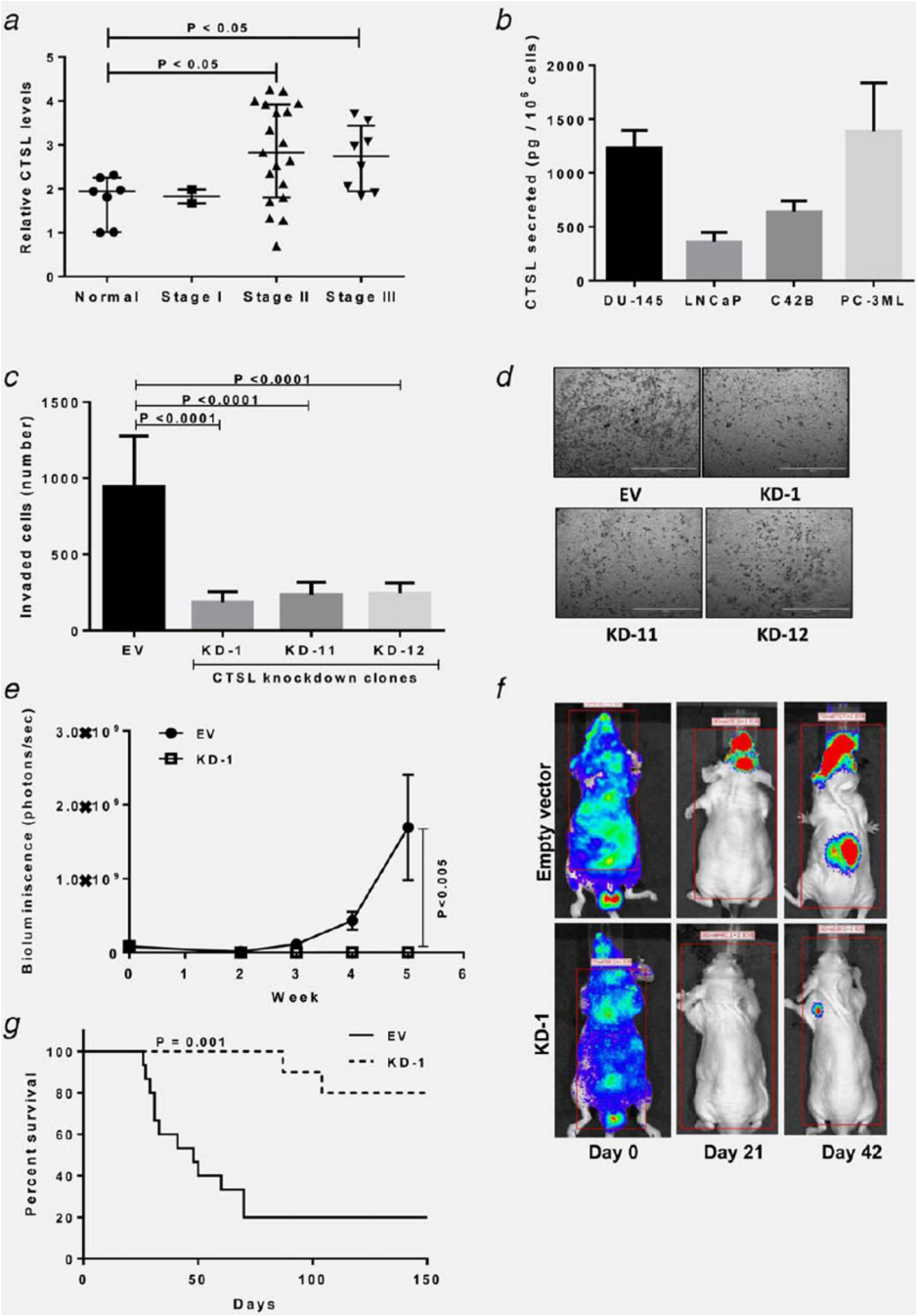

Figure 1.

CTSL ablation reduces metastatic disease burden. (***a***) CTSL semiquantitiative RT-PCR using Tissuescan prostate tissue panels. CTSL mRNA levels were normalized to β-actin. Line, median; whiskers, values at 25th and 75th percentiles; Mann-Whitney test. (***b***) CTSL secretion by metastatic prostate cancer cell lines. Bars represent means ± s.e.m from three independent experiments. (***c***) Invasion assay testing the effect of CTSL deficiency on the invasive capacity of PC-3ML cells. Bars represent means ± s.e.m from three independent experiments; Student's *t test*. (***d***) Representative images of invaded cells from c, scale bar= 2

mm. (***e***) *In vivo* bone metastasis assay. Measurement of bone metastasis burden based on bioluminescence intensity (photons per second); $n \geq 10$. Results are means ± s.e.m, analysis of variance. (***f***) Representative bioluminescence images of median mice inoculated with empty vector or CTSL shRNA transfected PC-3ML cells. (***g***) Kaplan-Meier survival curves of mice inoculated with empty vector of CTSL shRNA transfected PC-3ML cells; log-rank test.

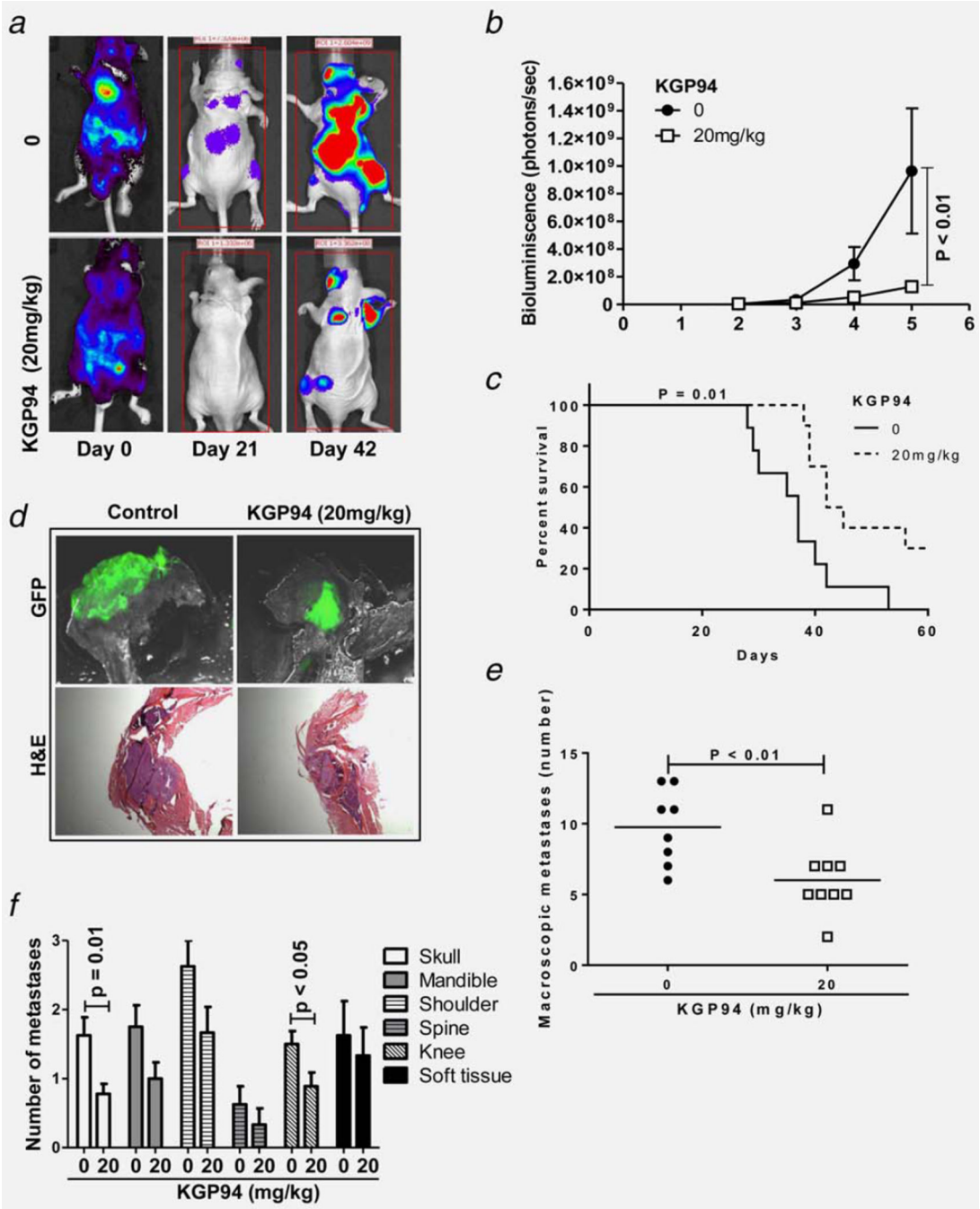

Figure 2.

KGP94 treatment decreases metastatic tumor burden and improves overall survival. (***a***) *In vivo* bone metastasis assay. Representative bioluminescence images of median mice from control and KGP94 treated cohorts. (***b***) Bone metastases burden in control and KGP94 treated mice measured based on photon flux (photons per second); $n \geq 8$. Results are means ± s.e.m, analysis of variance. (***c***) Kaplan-Meier survival curves of bone metastases bearing mice treated with or without 20 mg/kg KGP94; log-rank test. (***d***) Representative GFP and H&E images of bone metastases from each experimental group, scale bar= 1 mm. (***e***)

Number of macroscopic metastases in untreated and KGP94 treated mice; $n \geq 8$. Line, median; Mann-Whitney test. (***f***) Distribution of metastases by site.

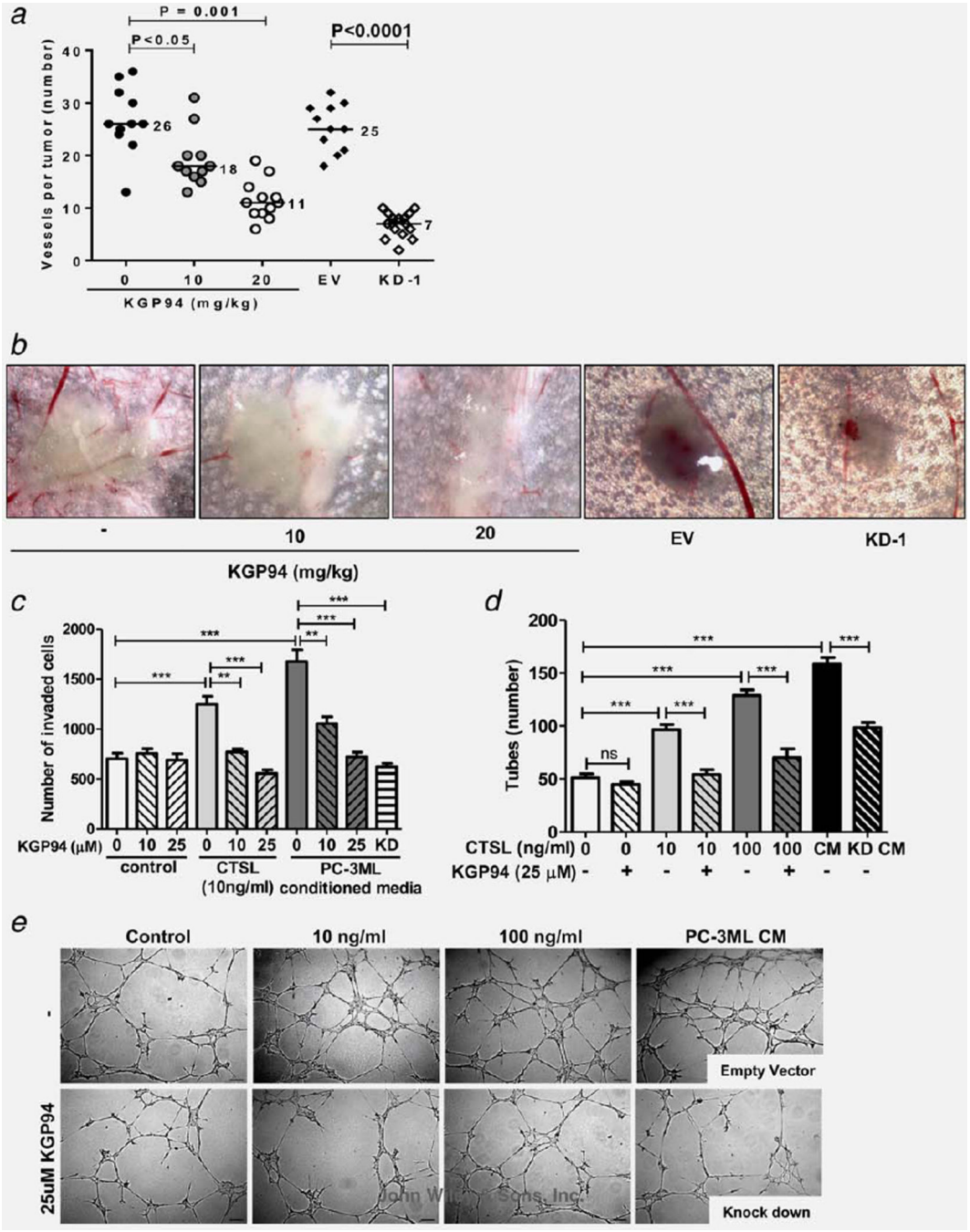

Figure 3.

CTSL inhibition suppresses prostate tumor angiogenesis. (***a***) Intradermal assay assessing the effect of pharmacological or genetic suppression of CTSL on PC-3ML tumor cell induced angiogenesis; $n \geq 11$. EV, empty vector; KD-1, CTSL knockdown PC-3ML tumor nodules; line, median; Mann-Whitney test. (***b***) Representative images of tumor nodules and blood vessels from a. (***c***) **, $p < 0.005$; ***, $p < 0.001$; Student's *t test*. (***d***) Effect of KGP94 on purified CTSL or conditioned media (CM) stimulated tube forming capacity of HMVEC-L

cells. KD CM, conditioned media from CTSL knockdown PC-3ML cells. ***, $p < 0.0001$, Student's *t test*. (***e***) Representative images from each experimental group shown in d.

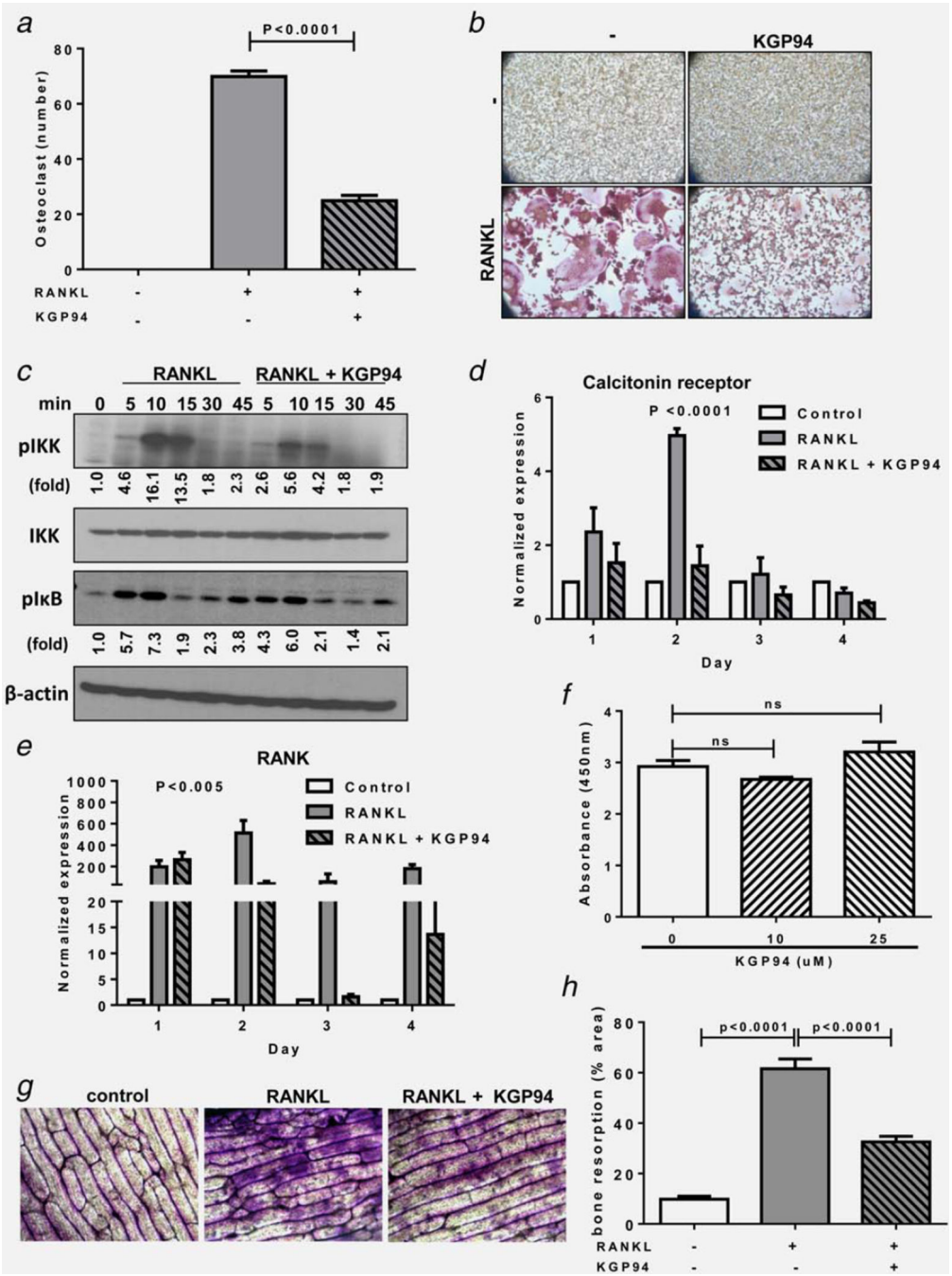

Figure 4.

KGP94 suppresses bone resorptive capacity of osteoclasts. (***a***) Quantification of TRAP+ multinucleate osteoclasts 4 days after stimulation with 35 ng/mL RANKL in the presence or absence of KGP94. Bars represent means ± s.e.m from three independent experiments; Student's *t* test. (***b***) Representative images from each experimental group. (***c***) Western blot analysis of the effect of KGP94 on RANKL stimulated NFκB pathway in RAW 264.7 cells. (***d*** and ***e***) Relative expression of osteoclastogenesis marker genes in RANKL stimulated RAW264.7 cells in the presence or absence of KGP94. Bars represent means ± s.e.m from

three independent experiments; analysis of variance. (***f***) Effect of KGP94 on osteoclast precursor cell viability; Student's *t* test. (***g***) Representative images of bone slices stained with O-toluidine to evaluate the extent of pit formation by osteoclasts under indicated conditions. (***h***) Percent area of bone resorbed by RANKL stimulated osteoclasts treated with or without KGP94. Results are means ± s.e.m from three independent experiments; Student's *t* test.

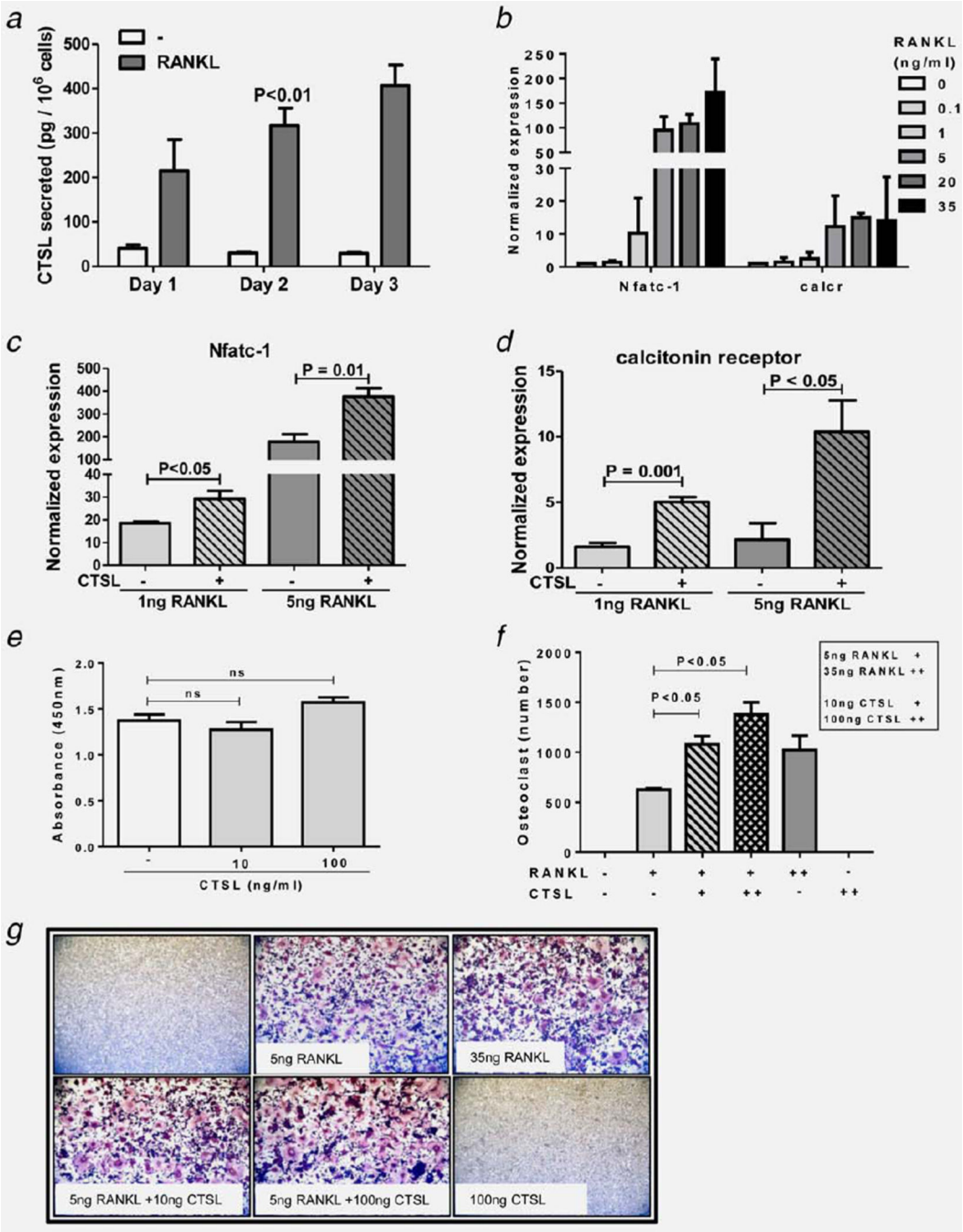

Figure 5.

CTSL promotes osteoclastogenesis. (***a***) Quantification of CTSL secretion by RAW 264.7 cells during the osteoclast formation process. (***b***) Dose response analysis of various concentrations of RANKL on the expression of osteoclastogenesis marker genes. (***c*** and ***d***) Effect of CTSL on RANKL stimulated osteoclastogenesis marker expression. Bars represent means ± s.e.m from three independent experiments, Student's *t* test. (***e***) Effect of purified CTSL on osteoclast precursor cell proliferation; Student's *t* test. (***f***) Quantification of TRAP + multinucleate osteoclasts 4 days after stimulation with indicated concentrations of purified

CTSL and RANKL. Bars represent means ± s.e.m from three independent experiments, Student's *t* test. (***g***) Representative images from each experimental group.

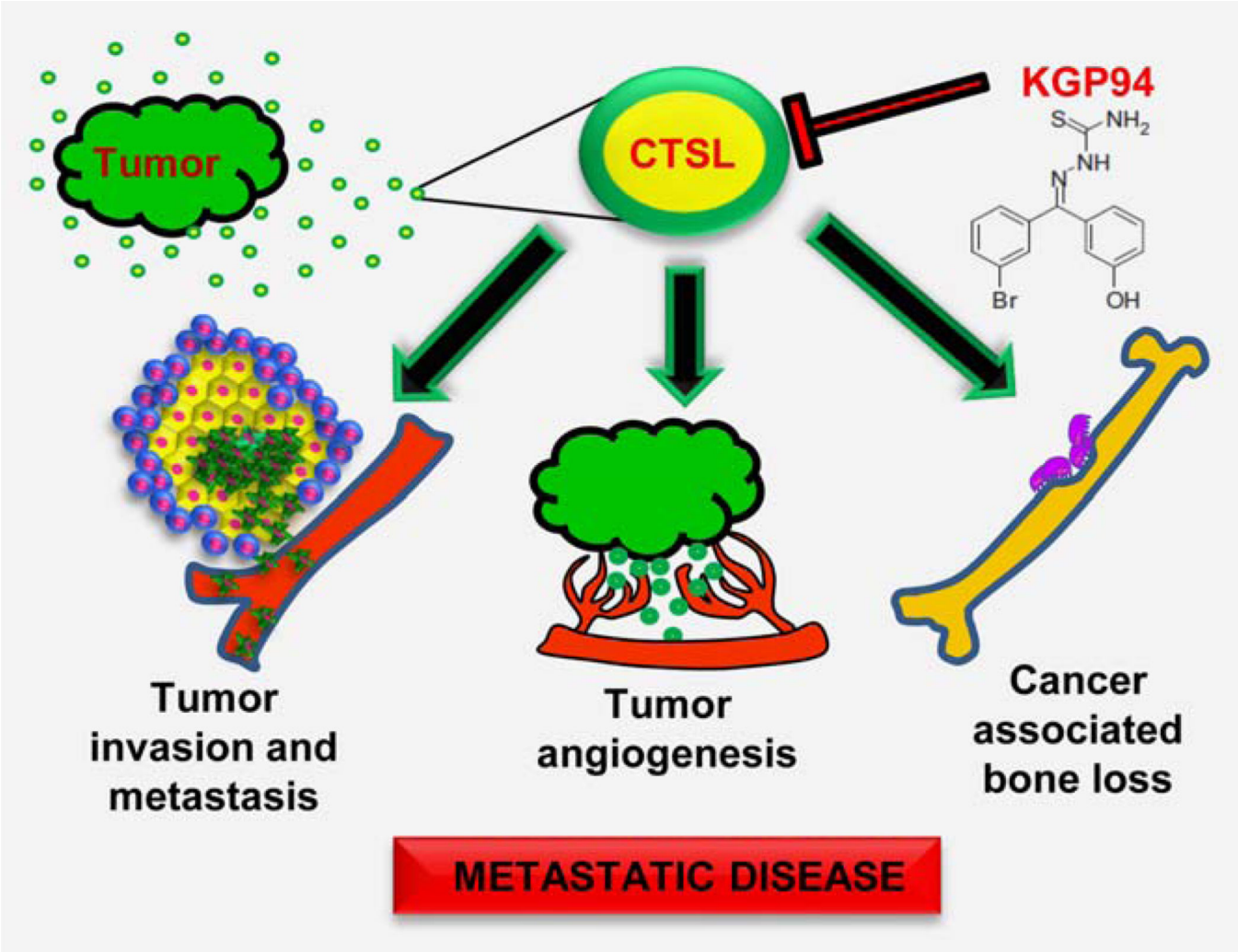

Figure 6.

Impact of CTSL on prostate cancer cell dissemination. Tumor secreted CTSL promotes metastatic progression by activating invasive cascades, stimulating tumor angiogenesis and fostering interaction between metastatic cells and the bone microenvironment. KGP94 mediated CTSL inactivation interferes with these processes and thus impairs metastatic disease progression and associated skeletal morbidities.